

# Fast Nonoverlapping Block Jacobi Method for the Dual Rudin–Osher–Fatemi Model\*

Chang-Ock Lee<sup>†</sup> and Jongho Park<sup>†</sup>

**Abstract.** We consider nonoverlapping domain decomposition methods for the Rudin–Osher–Fatemi (ROF) model, which is one of the standard models in mathematical image processing. The image domain is partitioned into rectangular subdomains and local problems in subdomains are solved in parallel. Local problems can adopt existing state-of-the-art solvers for the ROF model. We show that the nonoverlapping relaxed block Jacobi method for a dual formulation of the ROF model has the  $O(1/n)$  convergence rate of the energy functional, where  $n$  is the number of iterations. Moreover, by exploiting the forward-backward splitting structure of the method, we propose an accelerated version whose convergence rate is  $O(1/n^2)$ . The proposed method converges faster than existing domain decomposition methods both theoretically and practically, while the main computational cost of each iteration remains the same. We also provide the dependence of the convergence rates of the block Jacobi methods on the image size and the number of subdomains. Numerical results for comparisons with existing methods are presented.

**Key words.** Domain decomposition method, Block Jacobi method, Rudin–Osher–Fatemi model, Convergence rate, FISTA, Parallel computation

**AMS subject classifications.** 65N55, 65Y05, 65B99, 65K10, 68U10

**1. Introduction.** As large-scale images have become available in these days, it takes a long time to process such images and demands to reduce the time, especially in real time, are required. To accomplish such goal, there has been arisen the necessity of mathematical methods to make efficient use of distributed memory computers. In this perspective, we consider domain decomposition methods (DDMs), which have been already used successfully for elliptic partial differential equations [20, 24].

In DDMs, a large-scale problem defined on a domain  $\Omega$  is splitted into smaller ones called local problems defined on subdomains  $\{\Omega_s\}_{s=1}^N$  satisfying  $\bar{\Omega} = \bigcup_{s=1}^N \bar{\Omega}_s$ . We assign one local problem per processor so that all local problems can be solved in parallel in distributed memory computers. A solution of the full-dimension problem is obtained by the assembly of solutions of local problems. Thus, DDMs are suitable for distributed memory computers. Block Jacobi and Gauss–Seidel methods are typical examples of DDMs.

In this paper, we consider block Jacobi methods for the Rudin–Osher–Fatemi (ROF) model [22], which is one of the standard models in variational image processing given by

$$(1.1) \quad \min_{u \in BV(\Omega)} \left\{ \frac{\alpha}{2} \int_{\Omega} (u - f)^2 dx + TV(u) \right\},$$

where  $\alpha$  is a positive parameter,  $f$  is a corrupted image,  $TV(u)$  is the total variation of  $u$ , and

\*

**Funding:** This work was supported by NRF grant funded by MSIT (NRF-2017R1A2B4011627).

<sup>†</sup>Department of Mathematical Sciences, KAIST, Daejeon 34141, Korea  
(colee@kaist.edu, jongho.park@kaist.ac.kr).

$BV(\Omega)$  is the space of functions of bounded variation on an image domain  $\Omega \subset \mathbb{R}^2$ . There have been numerous approaches to solve (1.1); see [2, 5, 6, 12, 26, 27] for instance.

There have been several remarkable preceding researches on DDMs for variational image processing. Subspace correction methods for (1.1) were proposed in [10, 11], and various techniques to deal with local problems were considered in [15, 16]. In [13], subspace correction methods for the case of mixed  $L^1/L^2$ -fidelity were considered. However, it was shown in [17] that such subspace correction methods for (1.1) may not converge to a minimizer. To ensure convergence to a minimizer, in [8, 14, 17], subspace correction methods for the Fenchel–Rockafellar dual formulation of (1.1) given by

$$(1.2) \quad \min_{\mathbf{p} \in C_0^1(\Omega; \mathbb{R}^2)} \frac{1}{2} \int_{\Omega} (\operatorname{div} \mathbf{p} + \alpha f)^2 dx \quad \text{subject to } |\mathbf{p}(x)| \leq 1 \quad \forall x \in \Omega$$

were proposed, where  $C_0^1(\Omega; \mathbb{R}^2)$  is the set of continuously differentiable vector fields  $\mathbf{p}: \Omega \rightarrow \mathbb{R}^2$  with compact support. Recently, interface-based domain decomposition methods for total variation minimization were proposed [18, 19].

Over the past decade, block coordinate descent type algorithms for nonsmooth convex optimization have been successfully developed [3, 25]. They solve a minimization problem by successively minimizing the functional with respect to one of the coordinate blocks. In the context of domain decomposition methods, they correspond to nonoverlapping block Gauss–Seidel methods. Indeed, we observe that convergence rate analyses for block coordinate descent methods given in [7, 23] can be directly applied to the nonoverlapping block Gauss–Seidel method for (1.2) in [14]. However, to the best of our knowledge, there are no available analysis of the convergence rate for the nonoverlapping block Jacobi method for (1.2).

In this paper, we prove the  $O(1/n)$  convergence rate of the nonoverlapping relaxed block Jacobi method for (1.2), which was proposed in [14]. We note that it was shown in [8] that the overlapping counterpart is  $O(1/n)$  convergent and the authors gave a remark that their proof cannot be directly applied to the nonoverlapping case. In addition to the analysis of the convergence rate, we propose an accelerated nonoverlapping block Jacobi method for (1.2) which has the  $O(1/n^2)$  convergence rate. First, we modify the relaxed block Jacobi method so that it has the forward-backward splitting structure [9]. We call such a modified method as *pre-relaxed* block Jacobi method. Thanks to its forward-backward structure, we obtain an  $O(1/n^2)$  convergent algorithm by adding the momentum technique introduced in [2]. Numerical results ensure faster convergence of the proposed method compared to the existing ones.

The rest of the paper is organized as follows. Basic settings for the paper are presented in section 2. We analyze the convergence rate of the relaxed block Jacobi method and propose its variants including an  $O(1/n^2)$  convergent method in section 3. We consider how to deal with local problems of the proposed methods in section 4. We compare the proposed methods to the existing ones by numerical experiments in section 5. We conclude the paper with remarks in section 6.

**2. Preliminaries.** In this section, we review the standard finite difference framework for the ROF model. Then, we formulate the Fenchel–Rockafellar dual problem of the discrete ROF model. Finally, a nonoverlapping domain decomposition setting for the dual problem is presented. A list of notations used in sections 2 and 3 is given in Table 2.1.

notation	description	section
$\Omega$	image domain of size $M \times N$	2.1
$V$	a collection of functions: $\Omega \rightarrow \mathbb{R}$	2.1
$W$	a collection of functions: $\Omega \rightarrow \mathbb{R}^2$	2.1
$C$	$\{\mathbf{p} \in W :  \mathbf{p}_{ij}  \leq 1 \quad \forall (i, j) \in W\}$	2.1
$\nabla$	discrete gradient operator	2.1
$\text{div}$	discrete divergence operator, $\text{div} = -\nabla^*$	2.1
$F$	$F(\mathbf{p}) = \frac{1}{2} \ \text{div} \mathbf{p} + \alpha f\ _2^2$ , dual energy functional	2.1
$\chi_C$	characteristic function of $C \subset W$	2.1
$\mathcal{N}$	$M_s \times N_s$ , number of subdomains in the decomposition $\{\Omega_s\}_{s=1}^{\mathcal{N}}$	2.2
$N_c$	number of colors on the decomposition $\{\Omega_s\}_{s=1}^{\mathcal{N}}$	2.2
$S_k$	union of all subdomains with color $k$	2.2
$W_k$	a collection of functions: $S_k \rightarrow \mathbb{R}^2$	2.2
$R_k$	$R_k \mathbf{p} = \mathbf{p} _{S_k}$ , restriction operator: $W \rightarrow W_k$	2.2
$C_k$	$R_k C$	2.2
$F_k$	$F_k(\mathbf{p}_k; \mathbf{r}) = F(R_k^* \mathbf{p}_k + (I - R_k^* R_k) \mathbf{r})$ , local energy functional	2.2
$D_k$	Bregman distance associated with $F_k(\cdot; \mathbf{r})$	2.2
$D$	$D(\mathbf{p}, \mathbf{q}) = \sum_{k=1}^{N_c} D_k(R_k \mathbf{p}, R_k \mathbf{q})$	2.2
$S_k$	$S_k(\mathbf{p}) = \arg \min_{\mathbf{p}_k \in W_k} \{F_k(\mathbf{p}_k; \mathbf{p}) + \chi_{C_k}(\mathbf{p}_k)\}$	2.2
$\tilde{S}_k$	$\tilde{S}_k(\mathbf{p}) = R_k^* S_k(\mathbf{p}) + (I - R_k^* R_k) \mathbf{p}$	2.2
$\mathcal{P}_k$	$\mathcal{P}_k(\mathbf{p}) = \arg \min_{\mathbf{p}_k \in W_k} \{F_k(N_c \mathbf{p}_k - (N_c - 1) R_k \mathbf{p}; \mathbf{p}) + \chi_{C_k}(\mathbf{p}_k)\}$	3.2

Table 2.1

List of notations used in sections 2 and 3

**2.1. Discrete setting.** We assume that the grayscale image domain  $\Omega$  is composed of  $M \times N$  pixels; i.e.,

$$\Omega = \{(i, j) : 1 \leq i \leq M, 1 \leq j \leq N\}.$$

Let  $V$  and  $W$  be the collections of functions from  $\Omega$  into  $\mathbb{R}$  and  $\mathbb{R}^2$ , respectively. Both spaces are equipped with the usual Euclidean inner products  $\langle \cdot, \cdot \rangle$  and their induced norms  $\|\cdot\|_2$ . In addition, let  $C$  be the convex subset of  $W$  given by

$$C = \{\mathbf{p} \in W : |\mathbf{p}_{ij}| \leq 1 \quad \forall (i, j) \in \Omega\},$$

where  $|\mathbf{p}_{ij}| = (|p_{ij}^1|^2 + |p_{ij}^2|^2)^{1/2}$  for  $\mathbf{p} = (p^1, p^2)$ .

The discrete gradient operator  $\nabla: V \rightarrow W$  is defined by

$$\begin{aligned}
(\nabla u)_{ij}^1 &= \begin{cases} u_{i+1,j} - u_{ij} & \text{if } i = 1, \dots, M-1, \\ 0 & \text{if } i = M, \end{cases} \\
(\nabla u)_{ij}^2 &= \begin{cases} u_{i,j+1} - u_{ij} & \text{if } j = 1, \dots, N-1, \\ 0 & \text{if } j = N. \end{cases}
\end{aligned}$$

We define the discrete divergence operator  $\text{div}: W \rightarrow V$  as the minus adjoint of  $\nabla$ , i.e.,

$$(\text{div} \mathbf{p})_{ij} = \begin{cases} p_{ij}^1 & \text{if } i = 1, \\ p_{ij}^1 - p_{i-1,j}^1 & \text{if } i = 2, \dots, M-1, \\ -p_{i-1,j}^1 & \text{if } i = M \end{cases} + \begin{cases} p_{ij}^2 & \text{if } j = 1, \\ p_{ij}^2 - p_{i,j-1}^2 & \text{if } j = 2, \dots, N-1, \\ -p_{i,j-1}^2 & \text{if } j = N. \end{cases}$$

With the operators defined above, a discrete version of (1.1) is stated as

$$(2.1) \quad \min_{u \in V} \left\{ \frac{\alpha}{2} \|u - f\|_2^2 + \|\nabla u\|_1 \right\},$$

where  $\|\nabla u\|_1$  is the discrete total variation of  $u$  defined as the 1-norm of  $\nabla u$ :

$$\|\nabla u\|_1 = \sum_{(i,j) \in \Omega} |(\nabla u)_{ij}|.$$

Now, we consider the Fenchel–Rockafellar dual problem of (2.1). We define the energy functional  $F: W \rightarrow \mathbb{R}$  by

$$F(\mathbf{p}) = \frac{1}{2} \|\text{div} \mathbf{p} + \alpha f\|_2^2, \quad \mathbf{p} \in W.$$

It is well-known that a solution  $u^*$  of (2.1) can be recovered from a solution  $\mathbf{p}^*$  of

$$(2.2) \quad \min_{\mathbf{p} \in W} \{F(\mathbf{p}) + \chi_C(\mathbf{p})\}$$

by a simple algebraic formula

$$u^* = f + \frac{1}{\alpha} \text{div} \mathbf{p}^*.$$

Here  $\chi_C: W \rightarrow \bar{\mathbb{R}}$  is the characteristic function of  $C \subset W$  defined as

$$\chi_C(\mathbf{p}) = \begin{cases} 0 & \text{if } \mathbf{p} \in C, \\ \infty & \text{if } \mathbf{p} \notin C. \end{cases}$$

We call (2.2) the Fenchel–Rockafellar dual problem of (2.1). For more details, readers may refer [5, 21].

**2.2. Domain decomposition setting.** First, we partition the image domain  $\Omega$  into  $\mathcal{N} = M_s \times N_s$  nonoverlapping rectangular subdomains  $\{\Omega_s\}_{s=1}^{\mathcal{N}}$ . All subdomains can be classified into  $N_c$  classes (colors) by the usual coloring technique (see section 2.5.1 of [24]); local problems on subdomains in the same class are solved independently. Details of the coloring technique

will be given in [section 5](#). Let  $S_k$  be the union of all subdomains with color  $k$  for  $k = 1, \dots, N_c$ . Then, we have

$$\Omega = \bigcup_{k=1}^{N_c} S_k, \quad S_k \cap S_j = \emptyset \quad \forall k, j.$$

For each  $k = 1, \dots, N_c$ , we define the local function space  $W_k$  as the collection of functions from  $S_k$  to  $\mathbb{R}^2$ . Also, we define the restriction operator  $R_k: W \rightarrow W_k$  as

$$(2.3) \quad R_k \mathbf{p} = \mathbf{p}|_{S_k}, \quad \mathbf{p} \in W.$$

Then, its adjoint  $R_k^*: W_k \rightarrow W$  becomes the natural extension operator:

$$(R_k^* \mathbf{p}_k)_{ij} = \begin{cases} (\mathbf{p}_k)_{ij} & \text{if } (i, j) \in S_k, \\ \mathbf{0} & \text{if } (i, j) \notin S_k, \end{cases} \quad \mathbf{p}_k \in W_k.$$

Note that  $R_k^* R_k$  is the orthogonal projection from  $W$  onto  $W_k$  and

$$\sum_{k=1}^{N_c} R_k^* R_k = I.$$

We clearly have  $W = \bigoplus_{k=1}^{N_c} R_k^* W_k$ . Similarly, by defining  $C_k = R_k C$ , we have  $C = \bigoplus_{k=1}^{N_c} R_k^* C_k$  and

$$\chi_C(\mathbf{p}) = \sum_{k=1}^{N_c} \chi_{C_k}(R_k \mathbf{p}), \quad \mathbf{p} \in W.$$

Given  $\mathbf{r} \in W$ , the local energy functional  $F_k: W_k \rightarrow \mathbb{R}$  is defined as

$$F_k(\mathbf{p}_k; \mathbf{r}) = F(R_k^* \mathbf{p}_k + (I - R_k^* R_k) \mathbf{r}), \quad \mathbf{p}_k \in W_k.$$

The Bregman distance [\[4\]](#) associated with  $F_k(\cdot; \mathbf{r})$  is denoted by  $D_k$ , i.e.,

$$(2.4) \quad D_k(\mathbf{p}_k, \mathbf{q}_k) = F_k(\mathbf{p}_k; \mathbf{r}) - F_k(\mathbf{q}_k; \mathbf{r}) - \langle \nabla F_k(\mathbf{q}_k; \mathbf{r}), \mathbf{p}_k - \mathbf{q}_k \rangle, \quad \mathbf{p}_k, \mathbf{q}_k \in W_k,$$

and one can observe that it is independent of  $\mathbf{r}$ . Indeed, we have

$$(2.5) \quad D_k(\mathbf{p}_k, \mathbf{q}_k) = \frac{1}{2} \|\operatorname{div} R_k^* (\mathbf{p}_k - \mathbf{q}_k)\|_2^2.$$

We define the function  $D: W \times W \rightarrow \mathbb{R}$  as

$$(2.6) \quad D(\mathbf{p}, \mathbf{q}) = \sum_{k=1}^{N_c} D_k(R_k \mathbf{p}, R_k \mathbf{q}), \quad \mathbf{p}, \mathbf{q} \in W.$$

We provide the descent lemma corresponding to  $D$ .

**Lemma 2.1.** *For any  $\mathbf{p}, \mathbf{q} \in W$ , we have*

$$F(\mathbf{p}) \leq F(\mathbf{q}) + \langle \nabla F(\mathbf{q}), \mathbf{p} - \mathbf{q} \rangle + N_c D(\mathbf{p}, \mathbf{q}).$$

*Proof.* By direct calculation, we have

$$\begin{aligned} F(\mathbf{p}) - F(\mathbf{q}) - \langle \nabla F(\mathbf{q}), \mathbf{p} - \mathbf{q} \rangle &= \frac{1}{2} \|\operatorname{div}(\mathbf{p} - \mathbf{q})\|_2^2 \\ &= \frac{1}{2} \left\| \operatorname{div} \left( \sum_{k=1}^{N_c} R_k^* R_k (\mathbf{p} - \mathbf{q}) \right) \right\|_2^2 \\ &\leq N_c \sum_{k=1}^{N_c} \frac{1}{2} \|\operatorname{div} R_k^* R_k (\mathbf{p} - \mathbf{q})\|_2^2 = N_c D(\mathbf{p}, \mathbf{q}). \end{aligned}$$

■

Finally, we define two operators  $\mathcal{S}_k: W \rightarrow W_k$  and  $\bar{\mathcal{S}}_k: W \rightarrow W$  by

$$(2.7) \quad \mathcal{S}_k(\mathbf{p}) = \arg \min_{\mathbf{p}_k \in W_k} \{F_k(\mathbf{p}_k; \mathbf{p}) + \chi_{C_k}(\mathbf{p}_k)\}, \quad \mathbf{p} \in W,$$

and

$$\bar{\mathcal{S}}_k(\mathbf{p}) = R_k^* \mathcal{S}_k(\mathbf{p}) + (I - R_k^* R_k) \mathbf{p}, \quad \mathbf{p} \in W.$$

As the local energy functional  $F_k$  is not strongly convex, the minimization problem in (2.7) may admit nonunique minimizers. In this case, we take  $\mathcal{S}_k(\mathbf{p})$  as *any* one among them. By the optimality of  $\mathcal{S}_k$ , we have the following lemma.

**Lemma 2.2.** *For any  $\mathbf{p}_k \in C_k$  and  $\mathbf{q} \in C$ , we have*

$$F_k(\mathbf{p}_k; \mathbf{q}) - F(\bar{\mathcal{S}}_k(\mathbf{q})) \geq \frac{1}{2} \|\operatorname{div} R_k^* (\mathbf{p}_k - R_k \bar{\mathcal{S}}_k(\mathbf{q}))\|_2^2.$$

*Proof.* It is clear from the optimality condition of  $\mathcal{S}_k(\mathbf{q})$  (see the proof of Lemma 3.3 in [8]). ■

Lemma 2.2 shall be useful in the convergence analysis of block Jacobi methods in the next section. We note that it was also used in the case of overlapping domain decomposition [8].

**3. Block Jacobi methods.** In this section, we analyze the convergence rate of the relaxed block Jacobi method (Algorithm 2 in [14]) for (2.2). Then, by observing a resemblance between the relaxed block Jacobi method and the forward-backward splitting [2, 9], we propose a variant of the method called the pre-relaxed block Jacobi method, which has the exact forward-backward splitting structure. Based on the pre-relaxed block Jacobi method, we also propose an accelerated block Jacobi method which has the  $O(1/n^2)$  convergence rate.

**3.1. Relaxed Block Jacobi method.** The relaxed block Jacobi method for (2.2) is presented in the following, which was first proposed in [14].

**Algorithm 3.1** Relaxed Block Jacobi Method

---

Let  $\mathbf{p}^{(0)} \in C$ .  
**for**  $n = 0, 1, 2, \dots$   
 $\mathbf{p}^{(n+1)} = \frac{1}{N_c} \sum_{k=1}^{N_c} \bar{\mathcal{S}}_k(\mathbf{p}^{(n)})$   
**end**

---

Note that

$$\mathbf{p}^{(n+1)} = \frac{1}{N_c} \sum_{k=1}^{N_c} \bar{\mathcal{S}}_k(\mathbf{p}^{(n)}) = \left(1 - \frac{1}{N_c}\right) \mathbf{p}^{(n)} + \frac{1}{N_c} \sum_{k=1}^{N_c} R_k^* \mathcal{S}_k(\mathbf{p}^{(n)})$$

in [Algorithm 3.1](#). That is,  $\mathbf{p}^{(n+1)}$  is obtained by relaxation of  $\sum_{k=1}^{N_c} R_k^* \mathcal{S}_k(\mathbf{p}^{(n)})$  with  $\mathbf{p}^{(n)}$ , and it is the reason why we call [Algorithm 3.1](#) the relaxed block Jacobi method.

In [\[14\]](#), the convergence of [Algorithm 3.1](#) was shown without the convergence rate. It is summarized in the following proposition.

**Proposition 3.1.** *Let  $\{\mathbf{p}^{(n)}\}$  be the sequence generated by [Algorithm 3.1](#). Then, it satisfies the followings:*

- (i) *The sequence  $\{F(\mathbf{p}^{(n)})\}$  is decreasing, so that it converges.*
- (ii) *The sequence  $\{\mathbf{p}^{(n)}\}$  is bounded and has a limit point which is a solution of [\(2.2\)](#).*

First, we prove that the convergence rate of [Algorithm 3.1](#) is  $O(1/n)$ . The following lemma is a main ingredient for our proof.

**Lemma 3.2.** *For any  $\mathbf{p}, \mathbf{q} \in C$ , we have*

$$\frac{1}{N_c} F(\mathbf{p}) + \left(1 - \frac{1}{N_c}\right) F(\mathbf{q}) - F\left(\frac{1}{N_c} \sum_{k=1}^{N_c} \bar{\mathcal{S}}_k(\mathbf{q})\right) \geq D\left(\mathbf{p}, \frac{1}{N_c} \sum_{k=1}^{N_c} \bar{\mathcal{S}}_k(\mathbf{q})\right) - D(\mathbf{p}, \mathbf{q}).$$

*Proof.* For the sake of convenience, let

$$\mathcal{S}(\mathbf{q}) = \frac{1}{N_c} \sum_{k=1}^{N_c} \bar{\mathcal{S}}_k(\mathbf{q}).$$

By the convexity of  $F$ , we have

$$(3.1) \quad \frac{1}{N_c} \sum_{k=1}^{N_c} F(\bar{\mathcal{S}}_k(\mathbf{q})) \geq F(\mathcal{S}(\mathbf{q})).$$

Invoking [Lemma 2.2](#) with  $\mathbf{p}_k = R_k \mathbf{p}$  and summing over  $k = 1, \dots, N_c$  give

$$(3.2) \quad \frac{1}{N_c} \sum_{k=1}^{N_c} [F_k(R_k \mathbf{p}; \mathbf{q}) - F(\bar{\mathcal{S}}_k(\mathbf{q}))] \geq \frac{1}{N_c} \sum_{k=1}^{N_c} \frac{1}{2} \|\operatorname{div} R_k^* R_k (\mathbf{p} - \bar{\mathcal{S}}_k(\mathbf{q}))\|_2^2.$$

Also, by the relation

$$R_k^* R_k (\mathbf{p} - \mathcal{S}(\mathbf{q})) = \left(1 - \frac{1}{N_c}\right) R_k^* R_k (\mathbf{p} - \mathbf{q}) + \frac{1}{N_c} R_k^* R_k (\mathbf{p} - \bar{\mathcal{S}}_k(\mathbf{q}))$$

and the convexity of the functional  $\frac{1}{2} \|\operatorname{div} \cdot\|_2^2$ , we obtain

$$(3.3) \quad \frac{1}{2N_c} \|\operatorname{div} R_k^* R_k (\mathbf{p} - \bar{\mathcal{S}}_k(\mathbf{q}))\|_2^2 \geq \frac{1}{2} \|\operatorname{div} R_k^* R_k (\mathbf{p} - \mathcal{S}(\mathbf{q}))\|_2^2 - \frac{1}{2} \left(1 - \frac{1}{N_c}\right) \|\operatorname{div} R_k^* R_k (\mathbf{p} - \mathbf{q})\|_2^2.$$

Summation of (3.3) over  $k = 1, \dots, N_c$  yields

$$(3.4) \quad \frac{1}{N_c} \sum_{k=1}^{N_c} \frac{1}{2} \|\operatorname{div} R_k^* R_k (\mathbf{p} - \bar{\mathcal{S}}_k(\mathbf{q}))\|_2^2 \geq D(\mathbf{p}, \mathcal{S}(\mathbf{q})) - \left(1 - \frac{1}{N_c}\right) D(\mathbf{p}, \mathbf{q}).$$

On the other hand, we have

$$(3.5) \quad \begin{aligned} F(\mathbf{q}) - \frac{1}{N_c} \sum_{k=1}^{N_c} F_k(R_k \mathbf{p}; \mathbf{q}) &= \frac{1}{N_c} \sum_{k=1}^{N_c} [F(\mathbf{q}) - F(R_k^* R_k \mathbf{p} + (I - R_k^* R_k) \mathbf{q})] \\ &= \frac{1}{N_c} \sum_{k=1}^{N_c} \left[ -\langle \nabla F(\mathbf{q}), R_k^* R_k (\mathbf{p} - \mathbf{q}) \rangle - \frac{1}{2} \|\operatorname{div} R_k^* R_k (\mathbf{p} - \mathbf{q})\|_2^2 \right] \\ &= -\frac{1}{N_c} \langle \nabla F(\mathbf{q}), \mathbf{p} - \mathbf{q} \rangle - \frac{1}{N_c} D(\mathbf{p}, \mathbf{q}) \\ &\geq -\frac{1}{N_c} (F(\mathbf{p}) - F(\mathbf{q})) - \frac{1}{N_c} D(\mathbf{p}, \mathbf{q}), \end{aligned}$$

where the last inequality is due to the convexity of  $F$ . Summation of (3.1), (3.2), (3.4), and (3.5) yields the desired result.  $\blacksquare$

Now, we are ready to prove  $O(1/n)$  convergence of [Algorithm 3.1](#). The proof presented in this paper uses the same argument as the proof of Theorem 3.1 in [2].

**Theorem 3.3.** *Let  $\{\mathbf{p}^{(n)}\}$  be the sequence generated by [Algorithm 3.1](#) and  $\mathbf{p}^*$  be a solution of (2.2). Then, for any  $n \geq 1$ , we have*

$$F(\mathbf{p}^{(n)}) - F(\mathbf{p}^*) \leq \frac{N_c D(\mathbf{p}^*, \mathbf{p}^{(0)}) + (N_c - 1) (F(\mathbf{p}^{(0)}) - F(\mathbf{p}^*))}{n}.$$

*Proof.* Using [Lemma 3.2](#) with  $\mathbf{p} = \mathbf{p}^*$  and  $\mathbf{q} = \mathbf{p}^{(j)}$ , we get

$$\frac{1}{N_c} F(\mathbf{p}^*) + \left(1 - \frac{1}{N_c}\right) F(\mathbf{p}^{(j)}) - F(\mathbf{p}^{(j+1)}) \geq D(\mathbf{p}^*, \mathbf{p}^{(j+1)}) - D(\mathbf{p}^*, \mathbf{p}^{(j)}).$$

Summation of this inequality over  $j = 0, 1, \dots, n-1$  yields

$$(3.6) \quad \frac{n}{N_c} F(\mathbf{p}^*) + \left(1 - \frac{1}{N_c}\right) (F(\mathbf{p}^{(0)}) - F(\mathbf{p}^{(n)})) - \frac{1}{N_c} \sum_{j=1}^n F(\mathbf{p}^{(j)}) \geq D(\mathbf{p}^*, \mathbf{p}^{(n)}) - D(\mathbf{p}^*, \mathbf{p}^{(0)}).$$



Also, by Lemma 3.2 with  $\mathbf{p} = \mathbf{q} = \mathbf{p}^{(j)}$ , we obtain

$$F(\mathbf{p}^{(j)}) - F(\mathbf{p}^{(j+1)}) \geq D(\mathbf{p}^{(j)}, \mathbf{p}^{(j+1)}).$$

Multiplying this inequality by  $j$  and summing over  $j = 1, \dots, n-1$  yields

$$(3.7) \quad -nF(\mathbf{p}^{(n)}) + \sum_{j=1}^n F(\mathbf{p}^{(j)}) \geq \sum_{j=1}^{n-1} D(\mathbf{p}^{(j)}, \mathbf{p}^{(j+1)}).$$

Adding (3.6) times  $N_c$  and (3.7), we obtain

$$\begin{aligned} & n \left( F(\mathbf{p}^*) - F(\mathbf{p}^{(n)}) \right) + (N_c - 1) \left( F(\mathbf{p}^{(0)}) - F(\mathbf{p}^{(n)}) \right) \\ & \geq N_c \left( D(\mathbf{p}^*, \mathbf{p}^{(n)}) - D(\mathbf{p}^*, \mathbf{p}^{(0)}) \right) + \sum_{j=1}^{n-1} D(\mathbf{p}^{(j)}, \mathbf{p}^{(j+1)}). \end{aligned}$$

That is,

$$\begin{aligned} n \left( F(\mathbf{p}^*) - F(\mathbf{p}^{(n)}) \right) & \geq (N_c - 1) \left( F(\mathbf{p}^{(n)}) - F(\mathbf{p}^{(0)}) \right) \\ & \quad + N_c \left( D(\mathbf{p}^*, \mathbf{p}^{(n)}) - D(\mathbf{p}^*, \mathbf{p}^{(0)}) \right) + \sum_{j=1}^{n-1} D(\mathbf{p}^{(j)}, \mathbf{p}^{(j+1)}) \\ & \geq -(N_c - 1) \left( F(\mathbf{p}^{(0)}) - F(\mathbf{p}^*) \right) - N_c D(\mathbf{p}^*, \mathbf{p}^{(0)}). \end{aligned}$$

Therefore, we conclude that

$$F(\mathbf{p}^{(n)}) - F(\mathbf{p}^*) \leq \frac{N_c D(\mathbf{p}^*, \mathbf{p}^{(0)}) + (N_c - 1) (F(\mathbf{p}^{(0)}) - F(\mathbf{p}^*))}{n}.$$

*Remark 3.4.* In [8], the relaxed block Jacobi method with overlapping domain decomposition has  $O(1/n)$  convergence rate with the constant that tends to  $\infty$  as the overlapping size tends to 0. Therefore, the proof in [8] does not guarantee the convergence of the method in the nonoverlapping case.

By the definition of  $D(\mathbf{p}^*, \mathbf{p}^{(0)})$  in (2.6), the estimate given in Theorem 3.3 depends on the number of subdomains  $\mathcal{N}$ . The following lemma describes such dependency in detail.

*Lemma 3.5.* Assume that  $\Omega$  with  $M \times N$  pixels is partitioned into  $\mathcal{N} = M_s \times N_s$  nonoverlapping rectangular subdomains of the same size. For any  $\mathbf{p} \in W$ , we have

$$\sum_{k=1}^{N_c} \|\operatorname{div} R_k^* R_k \mathbf{p}\|_2^2 \leq \|\operatorname{div} \mathbf{p}\|_2^2 + c_1 \|\mathbf{p}\|_\infty^2,$$

where  $c_1$  is given by

$$(3.8) \quad c_1 = 7 \left( MN_s + M_s N - \frac{11}{7} M_s N_s \right).$$

*Proof.* For  $\mathbf{p} \in W$ , we define  $R^s \mathbf{p} = \mathbf{p}|_{\Omega_s}$  for  $s = 1, \dots, \mathcal{N}$ . Then, we clearly have

$$\sum_{k=1}^{N_c} \|\operatorname{div} R_k^* R_k \mathbf{p}\|_2^2 = \sum_{s=1}^{\mathcal{N}} \|\operatorname{div} (R^s)^* R^s \mathbf{p}\|_2^2.$$

For  $(i, j) \in \Omega$ , by the definition of  $\operatorname{div}$ , one requires  $\mathbf{p}_{ij}$ ,  $\mathbf{p}_{i-1,j}$ , and  $\mathbf{p}_{i,j-1}$  to compute  $(\operatorname{div} \mathbf{p})_{ij}$ . Let  $\tilde{\Omega}_s$  and  $\Omega_s^\circ$  be subsets of  $\Omega$  defined by

$$\tilde{\Omega}_s = \bigcup_{(i,j) \in \Omega_s} \{(i, j), (i+1, j), (i, j+1) \in \Omega\}$$

and

$$\Omega_s^\circ = \{(i, j) \in \Omega : (i, j), (i-1, j), (i, j-1) \in \Omega_s\},$$

respectively; see [Figure 3.1](#) for graphical description. Since

$$\mathbf{p} = (R^s)^* R^s \mathbf{p} \quad \text{in } \Omega_s,$$

one can observe that

$$\operatorname{supp} (\operatorname{div} (R^s)^* R^s \mathbf{p}) \subset \tilde{\Omega}_s$$

and

$$\operatorname{div} (R^s)^* R^s \mathbf{p} = \operatorname{div} \mathbf{p} \quad \text{in } \Omega_s^\circ.$$

Thus, we obtain that

$$\begin{aligned} & \|\operatorname{div} (R^s)^* R^s \mathbf{p}\|_2^2 - \|(\operatorname{div} \mathbf{p})|_{\Omega_s}\|_2^2 \\ & \leq \sum_{(i,j) \in \tilde{\Omega}_s \setminus \Omega_s} \left[ (\operatorname{div} (R^s)^* R^s \mathbf{p})_{ij} \right]^2 + \sum_{(i,j) \in \Omega_s \setminus \Omega_s^\circ} \left[ (\operatorname{div} (R^s)^* R^s \mathbf{p})_{ij} \right]^2 \\ (3.9) \quad & = \sum_{(i,j) \in E_1} (p_{ij}^1 + p_{ij}^2 - p_{i,j-1}^2)^2 + \sum_{(i,j) \in E_2} (-p_{i-1,j}^1)^2 \\ & \quad + \sum_{(i,j) \in E_3} (p_{ij}^1 - p_{i-1,j}^1 + p_{ij}^2)^2 + \sum_{(i,j) \in E_4} (-p_{i,j-1}^2)^2 + \sum_{(i,j) \in E_5} (p_{ij}^1 + p_{ij}^2)^2, \end{aligned}$$

where  $E_1, E_2, E_3, E_4$ , and  $E_5$  are regions indicated in [Figure 3.1\(c\)](#). Note that the cardinalities of these regions are  $\frac{N}{N_s} - 1$ ,  $\frac{N}{N_s}$ ,  $\frac{M}{M_s} - 1$ ,  $\frac{M}{M_s}$ , and 1, respectively. By the Cauchy–Schwarz inequality, we have

$$\begin{aligned} \sum_{(i,j) \in E_1} (p_{ij}^1 + p_{ij}^2 - p_{i,j-1}^2)^2 & \leq \sum_{(i,j) \in E_1} 3 [(p_{ij}^1)^2 + (p_{ij}^2)^2 + (p_{i,j-1}^2)^2] \\ & \leq \sum_{(i,j) \in E_1} 6 \|\mathbf{p}\|_\infty^2 = 6 \left( \frac{N}{N_s} - 1 \right) \|\mathbf{p}\|_\infty^2. \end{aligned}$$

Similarly, one obtains the followings:

$$\begin{aligned}
\sum_{(i,j) \in E_2} (-p_{i-1,j}^1)^2 &\leq \frac{N}{N_s} \|\mathbf{p}\|_\infty^2, \\
\sum_{(i,j) \in E_3} (p_{ij}^1 - p_{i-1,j}^1 + p_{ij}^2)^2 &\leq 6 \left( \frac{M}{M_s} - 1 \right) \|\mathbf{p}\|_\infty^2, \\
\sum_{(i,j) \in E_4} (-p_{i,j-1}^2)^2 &\leq \frac{M}{M_s} \|\mathbf{p}\|_\infty^2, \\
\sum_{(i,j) \in E_5} (p_{ij}^1 + p_{ij}^2)^2 &\leq \|\mathbf{p}\|_\infty^2.
\end{aligned}$$

Combining all inequalities stated above, we conclude that

$$\begin{aligned}
\|\operatorname{div}(R^s)^* R^s \mathbf{p}\|_2^2 - \|(\operatorname{div} \mathbf{p})|_{\Omega_s}\|_2^2 &\leq \left[ 6 \left( \frac{N}{N_s} - 1 \right) + \frac{N}{N_s} + 6 \left( \frac{M}{M_s} - 1 \right) + \frac{M}{M_s} + 1 \right] \|\mathbf{p}\|_\infty^2 \\
&= 7 \left( \frac{M}{M_s} + \frac{N}{N_s} - \frac{11}{7} \right) \|\mathbf{p}\|_\infty^2.
\end{aligned}$$

Summing the last inequality for  $s = 1, \dots, \mathcal{N}$  yields

$$\begin{aligned}
\sum_{s=1}^{\mathcal{N}} \|\operatorname{div}(R^s)^* R^s \mathbf{p}\|_2^2 - \|\operatorname{div} \mathbf{p}\|_2^2 &= \sum_{s=1}^{\mathcal{N}} (\|\operatorname{div}(R^s)^* R^s \mathbf{p}\|_2^2 - \|(\operatorname{div} \mathbf{p})|_{\Omega_s}\|_2^2) \\
&\leq 7M_s N_s \left( \frac{M}{M_s} + \frac{N}{N_s} - \frac{11}{7} \right) \|\mathbf{p}\|_\infty^2 \\
&= 7 \left( MN_s + M_s N - \frac{11}{7} M_s N_s \right) \|\mathbf{p}\|_\infty^2.
\end{aligned}$$

This completes the proof. ■

*Remark 3.6.* In the case of the stripe-shaped domain decomposition, say  $M_s = 1$  and  $N_s = \mathcal{N}$ , one may obtain a sharper estimate than [Lemma 3.5](#) since we do not need to deal with the terms related to  $E_1$  and  $E_2$  in [\(3.9\)](#). As a result, we obtain

$$\sum_{k=1}^{N_c} \|\operatorname{div} R_k^* R_k \mathbf{p}\|_2^2 \leq \|\operatorname{div} \mathbf{p}\|_2^2 + \mathcal{N}(7M - 5) \|\mathbf{p}\|_\infty^2.$$

As a direct consequence of [Lemma 3.5](#), we get the following upper bound for  $D(\mathbf{p}^*, \mathbf{p})$  for any  $\mathbf{p} \in C$ .

**Corollary 3.7.** *Let  $\mathbf{p}^*$  be a solution of [\(2.2\)](#). Then, for any  $\mathbf{p} \in C$ , we have*

$$D(\mathbf{p}^*, \mathbf{p}) \leq F(\mathbf{p}) - F(\mathbf{p}^*) + 2c_1,$$

where  $c_1$  is given in [\(3.8\)](#).

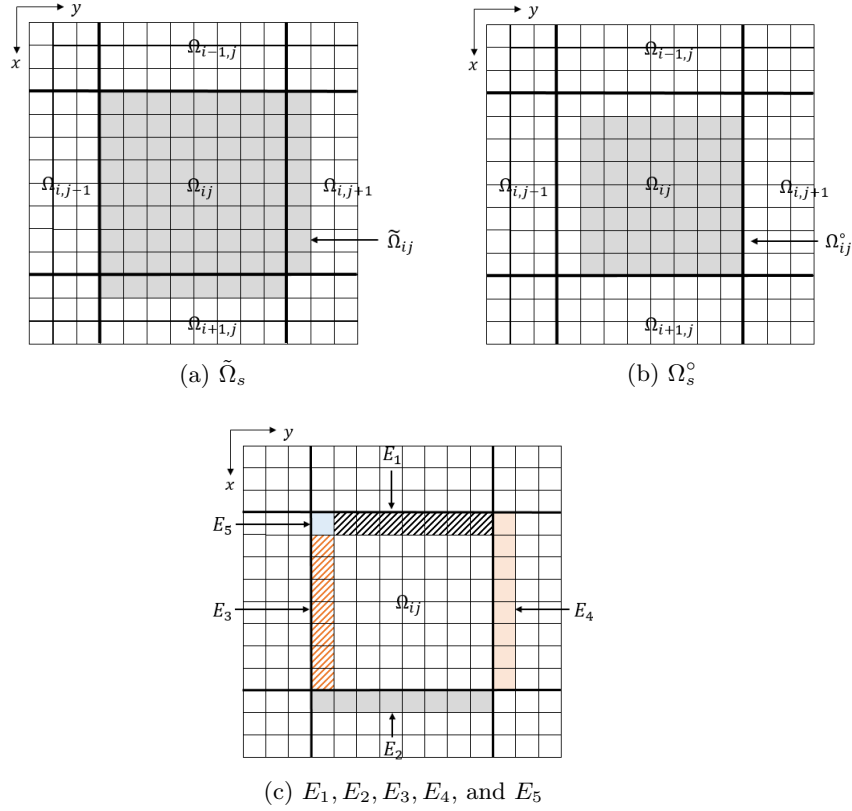


**Figure 3.1.** Subsets of  $\Omega$  introduced in the proof of Lemma 3.5

*Proof.* From the optimality condition of  $\mathbf{p}^*$ , we get

$$(3.10) \quad \frac{1}{2} \|\operatorname{div}(\mathbf{p} - \mathbf{p}^*)\|_2^2 \leq F(\mathbf{p}) - F(\mathbf{p}^*).$$

Also, since both  $\mathbf{p}$  and  $\mathbf{p}^*$  are in  $C$ , we have

$$(3.11) \quad \|\mathbf{p} - \mathbf{p}^*\|_\infty \leq 2.$$

With Lemma 3.5 and (3.10) and (3.11), we readily obtain

$$\begin{aligned} D(\mathbf{p}^*, \mathbf{p}) &= \frac{1}{2} \sum_{k=1}^{N_c} \|\operatorname{div} R_k^* R_k(\mathbf{p} - \mathbf{p}^*)\|_2^2 \\ &\leq \frac{1}{2} \|\operatorname{div}(\mathbf{p} - \mathbf{p}^*)\|_2^2 + \frac{c_1}{2} \|\mathbf{p} - \mathbf{p}^*\|_\infty^2 \\ &\leq F(\mathbf{p}) - F(\mathbf{p}^*) + 2c_1. \end{aligned}$$

■

Combining Theorem 3.3 and Corollary 3.7, we obtain the following estimate of convergence rate, in which dependence on the size of the image and the number of subdomains is revealed.

**Corollary 3.8.** Let  $\{\mathbf{p}^{(n)}\}$  be the sequence generated by [Algorithm 3.1](#) and  $\mathbf{p}^*$  be a solution of (2.2). Then, for any  $n \geq 1$ , we have

$$F(\mathbf{p}^{(n)}) - F(\mathbf{p}^*) \leq \frac{N_c}{n} \left[ \left( 2 - \frac{1}{N_c} \right) (F(\mathbf{p}^{(0)}) - F(\mathbf{p}^*)) + 2c_1 \right],$$

where  $c_1$  is given in (3.8).

**Remark 3.9.** One can obtain a relation between the convergence rate and the total length of the subdomain interfaces from [Corollary 3.8](#). Let  $\Gamma_{st} = \partial\Omega_s \cap \partial\Omega_t$  for  $s < t$  and  $\Gamma = \bigcup_{s < t} \Gamma_{st}$ . If the decomposition  $\{\Omega_s\}_{s=1}^N$  is of  $M_s \times N_s$ , it is clear that the length of  $\Gamma$  is given by

$$|\Gamma| = M(N_s - 1) + N(M_s - 1).$$

For fixed  $M$  and  $N$ ,  $c_1$  satisfies

$$(3.12) \quad c_1 \leq 7|\Gamma| + c_2,$$

where  $c_2$  is a constant independent of  $M_s$  and  $N_s$ . Therefore, it is expected that the convergence rate of [Algorithm 3.1](#) may deteriorate as  $|\Gamma|$  increases. Using [Remark 3.6](#), the same bound as (3.12) can be yielded for the stripe-shaped domain decomposition.

**3.2. Pre-relaxed Block Jacobi method.** First, we observe that [Lemma 3.2](#) has the similar form to one in the fundamental lemma of the forward-backward splitting (see [Lemma 2.3](#) of [2]):

$$(3.13) \quad F(\mathbf{p}) - F(\mathcal{T}(\mathbf{q})) \geq \frac{L}{2} (\|\mathbf{p} - \mathcal{T}(\mathbf{q})\|^2 - \|\mathbf{p} - \mathbf{q}\|^2), \quad \mathbf{p}, \mathbf{q} \in C,$$

where  $\mathcal{T}: W \rightarrow W$  is a certain operator which computes the next iterate of the algorithm, and  $L$  is a constant. If we replace  $F(\mathbf{p})$  in (3.13) by  $\frac{1}{N_c}F(\mathbf{p}) + \frac{N_c-1}{N_c}F(\mathbf{q})$ , then we obtain the formula in [Lemma 3.2](#). Note that an  $O(1/n)$  convergent algorithm with the forward-backward splitting (3.13) has the FISTA acceleration [2]. However, even though [Algorithm 1](#) has the  $O(1/n)$  convergence rate, it is difficult to apply the FISTA acceleration because of such differences. Since the relaxation step is crucial to guarantee the convergence of the algorithm [8], to apply the FISTA acceleration, we modify the algorithm so that a formula of the form (3.13) can be yielded while it still has the relaxation step.

We define an alternative local solution operator  $\mathcal{P}_k: W \rightarrow W_k$  by

$$(3.14) \quad \mathcal{P}_k(\mathbf{p}) = \arg \min_{\mathbf{p}_k \in W_k} \{F_k(N_c \mathbf{p}_k - (N_c - 1)R_k \mathbf{p}; \mathbf{p}) + \chi_{C_k}(\mathbf{p}_k)\}, \quad \mathbf{p} \in W.$$

The difference between two operators  $\mathcal{S}_k$  and  $\mathcal{P}_k$  is that,  $\mathbf{p}_k$  in  $\mathcal{S}_k$  is replaced by the relaxed term  $N_c \mathbf{p}_k - (N_c - 1)R_k \mathbf{p}$  in  $\mathcal{P}_k$ . Now, we propose a variant of [Algorithm 3.1](#) which uses  $\mathcal{P}_k$  as the local solution operator; see [Algorithm 3.2](#).

Compared to [Algorithm 3.1](#), the relaxation step is inside the local solution operator in [Algorithm 3.2](#). That is, the relaxation step is done *before* computing the local solution operator. This is why we call [Algorithm 3.2](#) the *pre-relaxed* block Jacobi method. The following

**Algorithm 3.2** Pre-relaxed Block Jacobi Method

---

Let  $\mathbf{p}^{(0)} \in C$ .  
**for**  $n = 0, 1, 2, \dots$   
 $\quad \mathbf{p}^{(n+1)} = \sum_{k=1}^{N_c} R_k^* \mathcal{P}_k(\mathbf{p}^{(n)})$   
**end**

---

lemma says that an application of the operator  $\sum_{k=1}^{N_c} R_k^* \mathcal{P}_k$  is in fact a proximal descent step with respect to a pseudometric

$$d(\mathbf{p}, \mathbf{q}) = \left( \sum_{k=1}^{N_c} \|\operatorname{div} R_k^* R_k(\mathbf{p} - \mathbf{q})\|_2^2 \right)^{\frac{1}{2}} = \sqrt{2D(\mathbf{p}, \mathbf{q})}, \quad \mathbf{p}, \mathbf{q} \in W.$$

**Lemma 3.10.** For  $\mathbf{q} \in C$ ,  $\sum_{k=1}^{N_c} R_k^* \mathcal{P}_k(\mathbf{q})$  is a solution of the minimization problem

$$(3.15) \quad \min_{\mathbf{p} \in W} \{F(\mathbf{q}) + \langle \nabla F(\mathbf{q}), \mathbf{p} - \mathbf{q} \rangle + N_c D(\mathbf{p}, \mathbf{q}) + \chi_C(\mathbf{p})\}.$$

*Proof.* For  $\mathbf{p}_k \in W_k$ , let

$$\begin{aligned} G_k(\mathbf{p}_k) &= F_k(N_c \mathbf{p}_k - (N_c - 1) R_k \mathbf{q}; \mathbf{q}) \\ &= \frac{1}{2} \|\operatorname{div}(R_k^*(N_c \mathbf{p}_k - (N_c - 1) R_k \mathbf{q}) + (I - R_k^* R_k) \mathbf{q}) + \alpha f\|_2^2. \end{aligned}$$

Let us define

$$(3.16) \quad A_k = R_k \operatorname{div}^* \operatorname{div} R_k^*, \quad A = \sum_{k=1}^{N_c} R_k^* A_k R_k.$$

Then, we have

$$\begin{aligned} \nabla G_k(\mathbf{p}_k) &= N_c R_k \operatorname{div}^* [\operatorname{div}(R_k^*(N_c \mathbf{p}_k - (N_c - 1) R_k \mathbf{q}) + (I - R_k^* R_k) \mathbf{q}) + \alpha f] \\ &= N_c [R_k \nabla F(\mathbf{q}) + N_c A_k(\mathbf{p}_k - R_k \mathbf{q})]. \end{aligned}$$

Thus, the optimality condition of (3.14) reads as

$$(3.17) \quad \langle R_k \nabla F(\mathbf{q}) + N_c A_k(\mathcal{P}_k(\mathbf{q}) - R_k \mathbf{q}), \mathbf{p}_k - \mathcal{P}_k(\mathbf{q}) \rangle \geq 0, \quad \mathbf{p}_k \in C_k.$$

Assembly of (3.17) for  $k = 1, \dots, N_c$  gives

$$(3.18) \quad \left\langle \nabla F(\mathbf{q}) + N_c A \left( \sum_{k=1}^{N_c} R_k^* \mathcal{P}_k(\mathbf{q}) - \mathbf{q} \right), \mathbf{p} - \sum_{k=1}^{N_c} R_k^* \mathcal{P}_k(\mathbf{q}) \right\rangle \geq 0, \quad \mathbf{p} \in C,$$

which is the optimality condition of (3.15). Therefore,  $\sum_{k=1}^{N_c} R_k^* \mathcal{P}_k(\mathbf{q})$  is a solution of (3.15). ■

Together with Lemmas 2.1 and 3.10, we obtain a formula for Algorithm 3.2 which has the exactly same form as (3.13). The fundamental lemma for Algorithm 3.2 is presented in the following.

**Lemma 3.11.** *For any  $\mathbf{p}, \mathbf{q} \in C$ , we have*

$$\frac{1}{N_c} F(\mathbf{p}) - \frac{1}{N_c} F\left(\sum_{k=1}^{N_c} R_k^* \mathcal{P}_k(\mathbf{q})\right) \geq D\left(\mathbf{p}, \sum_{k=1}^{N_c} R_k^* \mathcal{P}_k(\mathbf{q})\right) - D(\mathbf{p}, \mathbf{q}).$$

*Proof.* For the sake of convenience, we define  $A$  as in (3.16) and

$$\mathcal{P}(\mathbf{q}) = \sum_{k=1}^{N_c} R_k^* \mathcal{P}_k(\mathbf{q}).$$

Invoking Lemma 2.1 yields

$$(3.19) \quad F(\mathbf{p}) - F(\mathcal{P}(\mathbf{q})) \geq F(\mathbf{p}) - F(\mathbf{q}) - \langle \nabla F(\mathbf{q}), \mathcal{P}(\mathbf{q}) - \mathbf{q} \rangle - N_c D(\mathcal{P}(\mathbf{q}), \mathbf{q}).$$

By Lemma 3.10,  $\mathcal{P}(\mathbf{q})$  satisfies (3.18), that is,

$$(3.20) \quad \langle \nabla F(\mathbf{q}) + N_c A(\mathcal{P}(\mathbf{q}) - \mathbf{q}), \mathbf{p} - \mathcal{P}(\mathbf{q}) \rangle \geq 0.$$

Also, by the convexity of  $F$ , we have

$$(3.21) \quad F(\mathbf{p}) \geq F(\mathbf{q}) + \langle \nabla F(\mathbf{q}), \mathbf{p} - \mathbf{q} \rangle.$$

Then, we get the desired result by summation of (3.19)–(3.21). ■

Since Lemma 3.11 has exactly the same form as Lemma 2.3 of [2], analysis of the  $O(1/n)$  convergence rate is straightforward.

**Theorem 3.12.** *Let  $\{\mathbf{p}^{(n)}\}$  be the sequence generated by Algorithm 3.2 and  $\mathbf{p}^*$  be a solution of (2.2). Then, for any  $n \geq 1$ , we have*

$$F(\mathbf{p}^{(n)}) - F(\mathbf{p}^*) \leq \frac{N_c}{n} \left[ F(\mathbf{p}^{(0)}) - F(\mathbf{p}^*) + 2c_1 \right],$$

where  $c_1$  is given in (3.8).

*Proof.* In Theorem 3.1 of [2], we replace  $L(f)$  and  $\|\cdot\|$  by  $N_c$  and

$$\|\cdot\| = \left( \sum_{k=1}^{N_c} \|\operatorname{div} R_k^* R_k(\cdot)\|_2^2 \right)^{\frac{1}{2}},$$

respectively, the notations we use. Consequently, we have the following estimate:

$$(3.22) \quad F(\mathbf{p}^{(n)}) - F(\mathbf{p}^*) \leq \frac{N_c D(\mathbf{p}^*, \mathbf{p}^{(0)})}{n}.$$

Application of Corollary 3.7 to (3.22) yields the desired result. ■

*Remark 3.13.* In [Theorem 3.12](#), we gave a little sharper bound than [Theorem 3.3](#). Indeed, our numerical experiments presented in [section 5](#) will show that [Theorem 3.12](#) has a faster energy decay than [Theorem 3.3](#) at initial dozens of iterations.

In addition, an accelerated version of [Algorithm 3.2](#) with the  $O(1/n^2)$  convergence rate can be designed by the same way as FISTA [\[2\]](#). It is summarized in [Algorithm 3.3](#).

---

**Algorithm 3.3** Fast Pre-relaxed Block Jacobi Method

---

Let  $\mathbf{p}^{(0)} = \mathbf{q}^{(0)} \in C$  and  $t_0 = 1$ .  
**for**  $n = 0, 1, 2, \dots$   
 $\mathbf{p}^{(n+1)} = \sum_{k=1}^{N_c} R_k^* \mathcal{P}_k \mathbf{q}^{(n)}$   
 $t_{n+1} = \frac{1 + \sqrt{1 + 4t_n^2}}{2}$   
 $\mathbf{q}^{(n+1)} = \mathbf{p}^{(n+1)} + \frac{t_n - 1}{t_{n+1}} (\mathbf{p}^{(n+1)} - \mathbf{p}^{(n)})$   
**end**

---

Finally, we state the convergence theorem for [Algorithm 3.3](#). [Theorem 3.14](#) says that [Algorithm 3.3](#) is superior to [Algorithms 3.1](#) and [3.2](#). In [section 5](#), we will present some numerical examples where [Algorithm 3.3](#) shows better performance than others.

*Theorem 3.14.* Let  $\{\mathbf{p}^{(n)}\}$  be the sequence generated by [Algorithm 3.3](#) and  $\mathbf{p}^*$  be a solution of [\(2.2\)](#). Then, for any  $n \geq 1$ , we have

$$F(\mathbf{p}^{(n)}) - F(\mathbf{p}^*) \leq \frac{4N_c}{(n+1)^2} \left[ F(\mathbf{p}^{(0)}) - F(\mathbf{p}^*) + 2c_1 \right],$$

where  $c_1$  is given in [\(3.8\)](#).

*Proof.* With the same argument as in [Theorem 4.4](#) of [\[2\]](#), we obtain

$$(3.23) \quad F(\mathbf{p}^{(n)}) - F(\mathbf{p}^*) \leq \frac{4N_c D(\mathbf{p}^*, \mathbf{p}^{(0)})}{(n+1)^2}.$$

Then, application of [Corollary 3.7](#) to [\(3.23\)](#) completes the proof. ■

*Remark 3.15.* In [Theorem 3.14](#), the  $O(1/n^2)$  convergence is satisfied regardless of  $f$  and  $\alpha$  since they only affect on  $F$ . That is, neither the noise level of a given image nor the value of the weight parameter  $\alpha$  interferes with the  $O(1/n^2)$  convergence of [Algorithm 3.3](#). Similar arguments apply to [Algorithms 3.1](#) and [3.2](#).

**4. Local problems.** In this section, we discuss how to deal with local problems of the block Jacobi methods introduced in this paper. The coloring technique used in the proposed methods is also considered.

First, we assume that the domain decomposition  $\{\Omega_s\}_{s=1}^{\mathcal{N}}$  is of the window shape as shown in [Figure 4.1\(a\)](#). All subdomains  $\Omega_s$  have the same size. Let  $\Omega_{ij}$  be the subdomain on the  $i$ -th row and the  $j$ -th column. We define the local function space  $W^s$  as the collection of functions



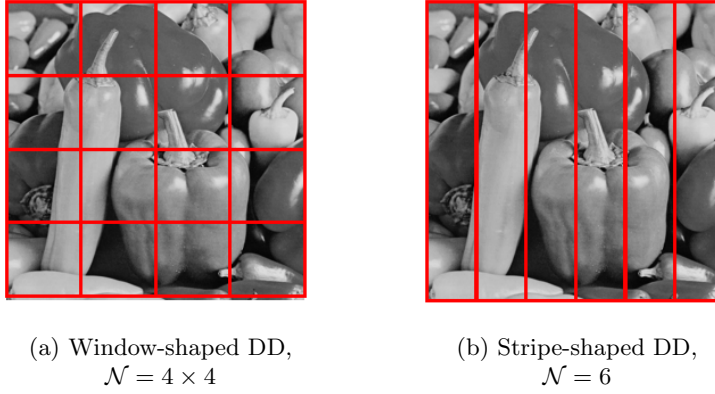


**Figure 4.1.** Two different shapes of domain decomposition

from  $\Omega_s$  to  $\mathbb{R}^2$ . Also, we define the restriction operator  $R^s: W \rightarrow W^s$  similarly to (2.3) and  $C^s = R^s C$ .

Local problems in  $\Omega_s$  have the following general form:

$$(4.1) \quad \min_{\mathbf{p}_s \in W^s} \frac{1}{2} \|\operatorname{div}(R^s)^* \mathbf{p}_s + g\|_2^2 + \chi_{C^s}(\mathbf{p}_s)$$

for some  $g \in V$ . Let  $\tilde{\Omega}_s$  be the subset of  $\Omega$  containing  $\Omega_s$  and its adjacent lines of pixels on the bottom and the right sides; see Figure 3.1(a). Also, we define  $\tilde{V}^s$  as the collection of functions from  $\tilde{\Omega}_s$  to  $\mathbb{R}$ . One can observe that  $\operatorname{div}(R^s)^* \mathbf{p}_s \in \tilde{V}_s$  for all  $\mathbf{p}_s \in W^s$ . Thus, it is natural to define the local divergence operator  $\operatorname{div}_s: W^s \rightarrow \tilde{V}^s$  by

$$(4.2) \quad \operatorname{div}_s \mathbf{p}_s = \operatorname{div}(R^s)^* \mathbf{p}_s, \quad \mathbf{p}_s \in W^s,$$

and the local gradient operator  $\nabla_s: \tilde{V}^s \rightarrow W^s$  by  $\nabla_s = -\operatorname{div}_s^*$ . With these local operators, it is straightforward to obtain the equivalent primal and primal-dual form of (4.1) as follows (see, for example, [21] for details):

$$(4.3a) \quad \min_{\tilde{u}_s \in \tilde{V}^s} \left\{ \frac{1}{2} \|\tilde{u}_s - g\|_2^2 + \|\nabla_s \tilde{u}_s\|_1 \right\},$$

$$(4.3b) \quad \min_{\tilde{u}_s \in \tilde{V}^s} \max_{\mathbf{p}_s \in W^s} \left\{ \langle \nabla_s \tilde{u}_s, \mathbf{p}_s \rangle + \frac{1}{2} \|\tilde{u}_s - g\|_2^2 - \chi_{C^s}(\mathbf{p}_s) \right\}.$$

Consequently, existing state-of-the-art solvers for the ROF model can be adopted for local problems of the proposed methods. For instance, one may solve (4.1) by FISTA [2], (4.3a) by the augmented Lagrangian method [27], or (4.3b) by the first order primal-dual algorithm [6].

Next, we consider the coloring technique used in the proposed methods. As we mentioned above, we assign the same color to subdomains if local problems associated to them are solved independently. To compute  $g \in \tilde{V}^s$  in (4.1), we require the values of  $\mathbf{q} \in W$  in the area marked

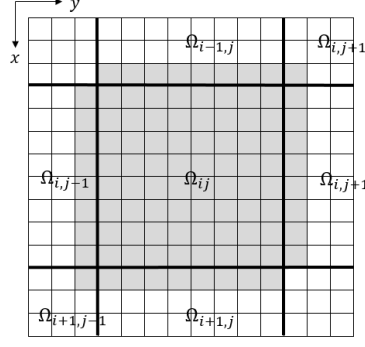


**Figure 4.2.** Local problem (4.1) is dependent on the degrees of freedom in the marked area.

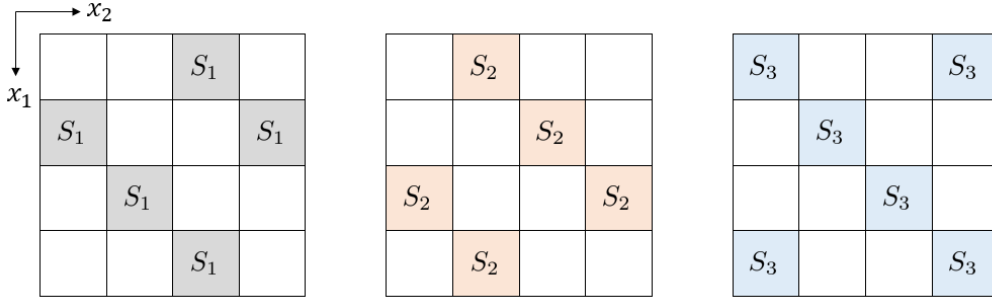


**Figure 4.3.** Domain decomposition with the coloring technique,  $N_c = 3$

in Figure 4.2, i.e.,  $\tilde{\Omega}_s$  plus its adjacent lines of pixels on the top and the left sides. It means that the local problem (4.1) on  $\Omega_{ij}$  is dependent on  $\Omega_{i-1,j}$ ,  $\Omega_{i-1,j+1}$ ,  $\Omega_{i,j-1}$ ,  $\Omega_{i,j+1}$ ,  $\Omega_{i+1,j-1}$ , and  $\Omega_{i+1,j}$ . Only  $\Omega_{i-1,j-1}$  and  $\Omega_{i+1,j+1}$  can have the same color as  $\Omega_{ij}$  among its neighboring subdomains. It can be accomplished with 3 colors; each subdomain  $\Omega_{ij}$  is colored with the color  $(i - j) \bmod 3$ . See Figure 4.3 for visual description. We notice that the same coloring technique was introduced in [17] for primal DDMs.

We conclude the section with a remark on domain decomposition shapes. Since DDMs are designed for use on distributed memory computers, it is important to reduce the amount of communications among processors. In this sense, the window-shaped domain decomposition shown in Figure 4.1(a) is most efficient because the total length of the subdomain interfaces is minimized. Moreover, we observed in (3.12) that the convergence rate of block Jacobi methods rely on the length of the subdomain interfaces. However, in the case when we have only a few number of processors, the stripe-shaped domain decomposition shown in Figure 4.1(b) can be a good alternative. Since the stripe-shaped domain decomposition can be colored with only 2 colors, one may expect better convergence rate; recall that all the convergence theorems presented in this paper are dependent on the number of colors  $N_c$ . Numerical comparison between two types of domain decomposition will be presented in the next section.

**5. Numerical experiments.** In this section, we present numerical results for the block Jacobi methods introduced in this paper. All codes were programmed using ANSI C with

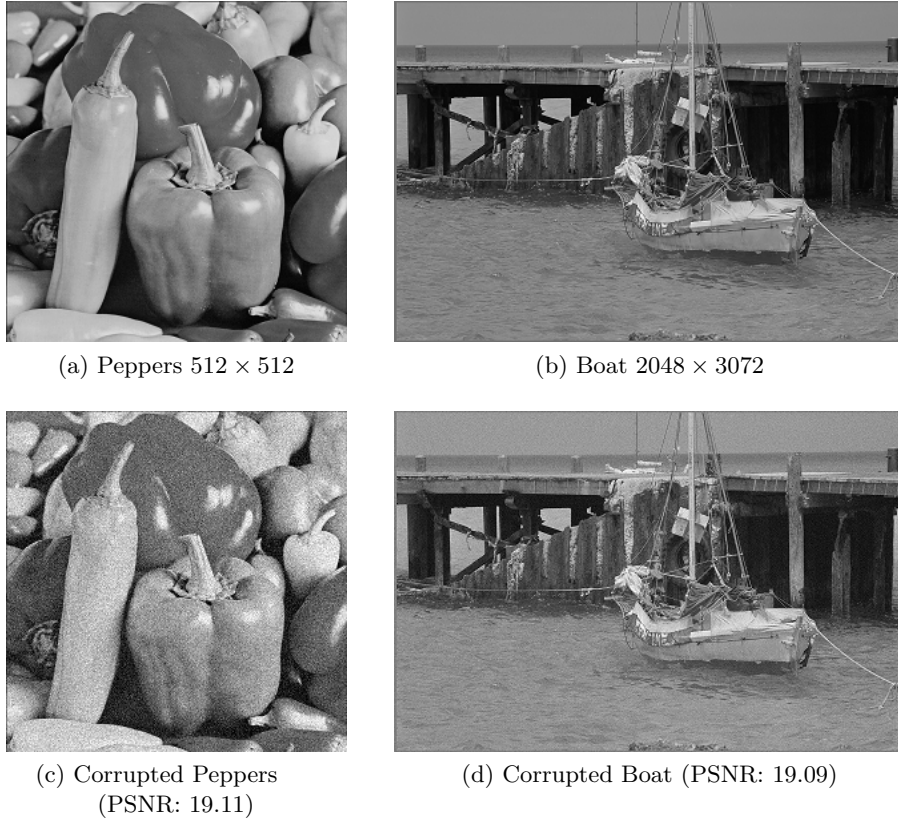


**Figure 5.1.** *Test images for the numerical experiments*

OpenMPI and compiled by Intel Parallel Studio XE. All computations were performed on a computer cluster composed of seven machines, where each machine is equipped with two Intel Xeon SP-6148 CPUs (2.4GHz, 20C), 192GB RAM, and the operating system CentOS 7.4 64bit. Two test images “Peppers  $512 \times 512$ ” and “Boat  $2048 \times 3072$ ” are used in our numerical experiments. Both are corrupted with additive Gaussian noise with mean 0 and variance 0.05; see Figure 5.1. As a measurement of the quality of denoising, we use the peak-signal-to-noise ratio (PSNR) defined by

$$\text{PSNR} = 10 \log_{10} \left( \frac{\text{MAX}^2 \cdot |\Omega|}{\|u - f_{\text{orig}}\|_2^2} \right),$$

where  $\text{MAX} = 1$  is the possible maximum value of pixel intensity and  $f_{\text{orig}}$  is the original clean image. The weight parameter  $\alpha$  in (2.2) is chosen as 5, 10, and 20 in our experiments.

For all experiments, we set the initial guess as  $\mathbf{p}^{(0)} = \mathbf{0}$ . To reduce the time elapsed in solving local problems, the local solutions  $\mathbf{p}_s^{(n-1)}$  from the previous iteration are chosen as initial guesses for the local problems at each iteration.

First, we compare the energy decay of several block methods: relaxed block Jacobi (Algorithm 3.1, RJ), block Gauss–Seidel (Algorithm 1 in [14], GS), pre-relaxed block Jacobi (Al-

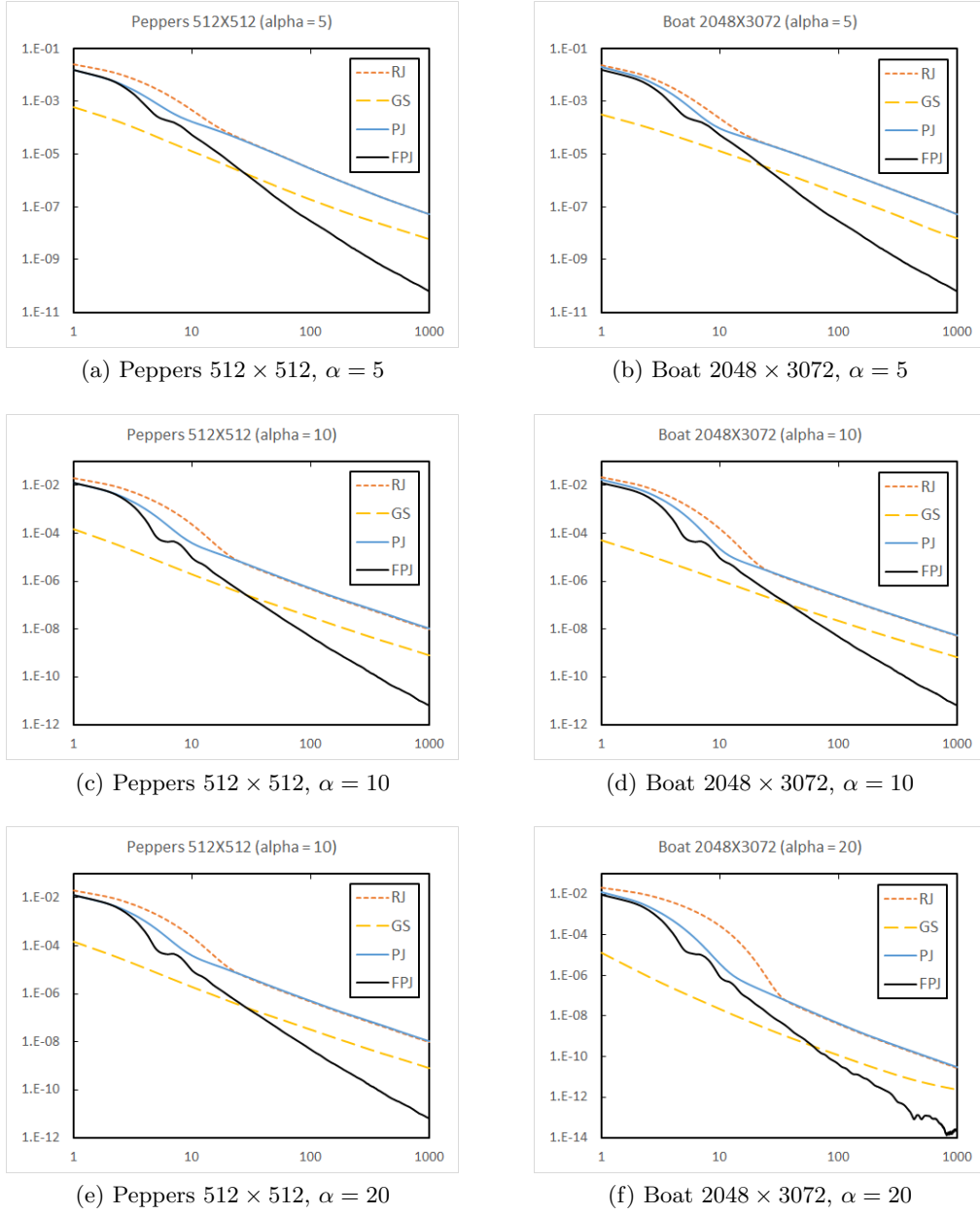


**Figure 5.2.** Decay of  $\frac{F(\mathbf{p}^{(n)}) - F(\mathbf{p}^*)}{F(\mathbf{p}^*)}$  in several block methods ( $\mathcal{N} = 8 \times 8$ )

gorithm 3.2, PJ), and fast pre-relaxed block Jacobi (Algorithm 3.3, FPJ) methods. Figure 5.2 plots  $\frac{F(\mathbf{p}^{(n)}) - F(\mathbf{p}^*)}{F(\mathbf{p}^*)}$  of the block methods per iteration in log-log scale, where  $\mathbf{p}^*$  is a solution of the full-dimension problem (2.2) obtained by  $10^6$  FISTA [2] iterations. The number of

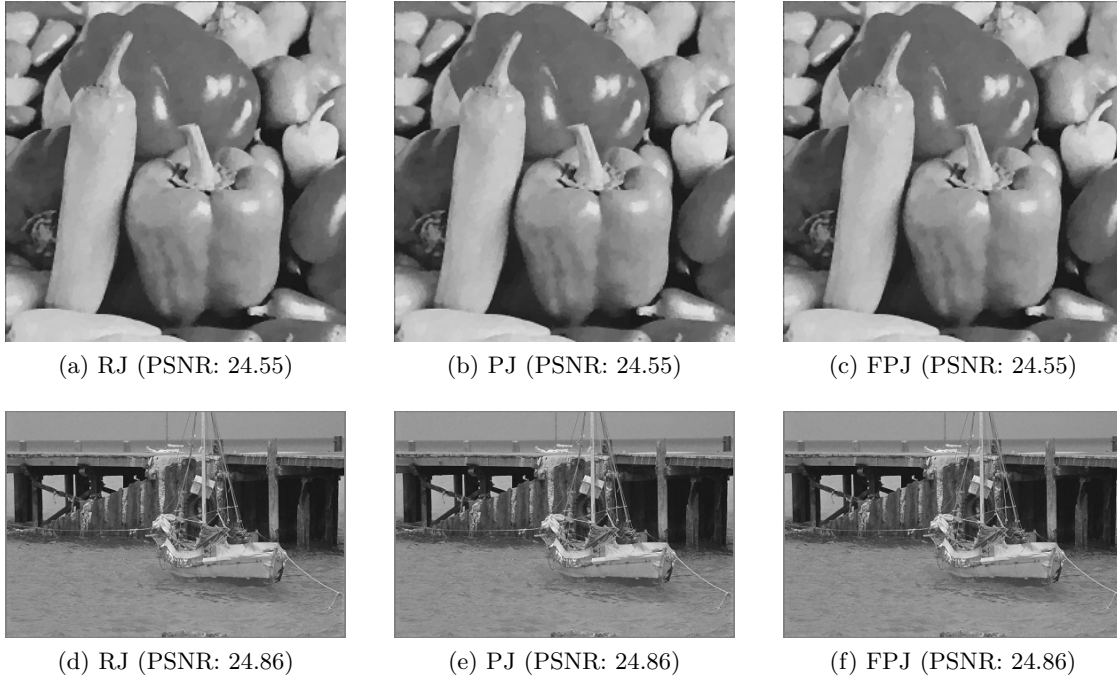


**Figure 5.3.** Results of the block Jacobi methods ( $\mathcal{N} = 8 \times 8$ ,  $\alpha = 10$ )

subdomains  $\mathcal{N}$  is fixed as  $8 \times 8$ . Local problems were solved by FISTA with the stop criterion

$$\frac{\|\operatorname{div}_s \mathbf{p}_s^{(n+1)} - \operatorname{div}_s \mathbf{p}_s^{(n)}\|_2}{\|\operatorname{div}_s \mathbf{p}_s^{(n+1)}\|_2} < 10^{-9} \quad \text{or} \quad n = 50,$$

where the operator  $\operatorname{div}_s$  was defined in (4.2). The above criterion was chosen so that stagnations of the energy do not occur (see Figure 5 in [19]). As we justified theoretically in section 3, the energy functional of FPJ converges to the minimum much faster than other methods. As noted in Remark 3.15, such fast convergence occurs regardless of the given image  $f$  and the weight parameter  $\alpha$ . In particular, the convergence rate of FPJ is faster than that of GS, while other block Jacobi methods converge more slowly than GS. We notice that the  $O(1/n)$  convergence of GS can be deduced as a direct consequence of [7, 23]. It is observed that the energy decay of FPJ is not monotone. This is due to the nature of FISTA, and one may use MFISTA [1] instead of FISTA acceleration to ensure monotone decay of the energy. Note that the monotonicity of MFISTA given in Appendix A of [1] can be applied to our framework directly. Interestingly, as we mentioned in Remark 3.13, PJ seems to be faster than RJ at first 20 iterations, but eventually shows similar convergence results compared to RJ in our numerical experiments. Meanwhile, as shown in Figure 5.3, all the results from three block Jacobi methods with  $\alpha = 10$  have the same PSNR and are not visually distinguishable. The same applies to the cases  $\alpha = 5, 20$ , and we omit the results for those cases.

For practical use in image restoration, the stop criteria need not be too strict; see [8] for

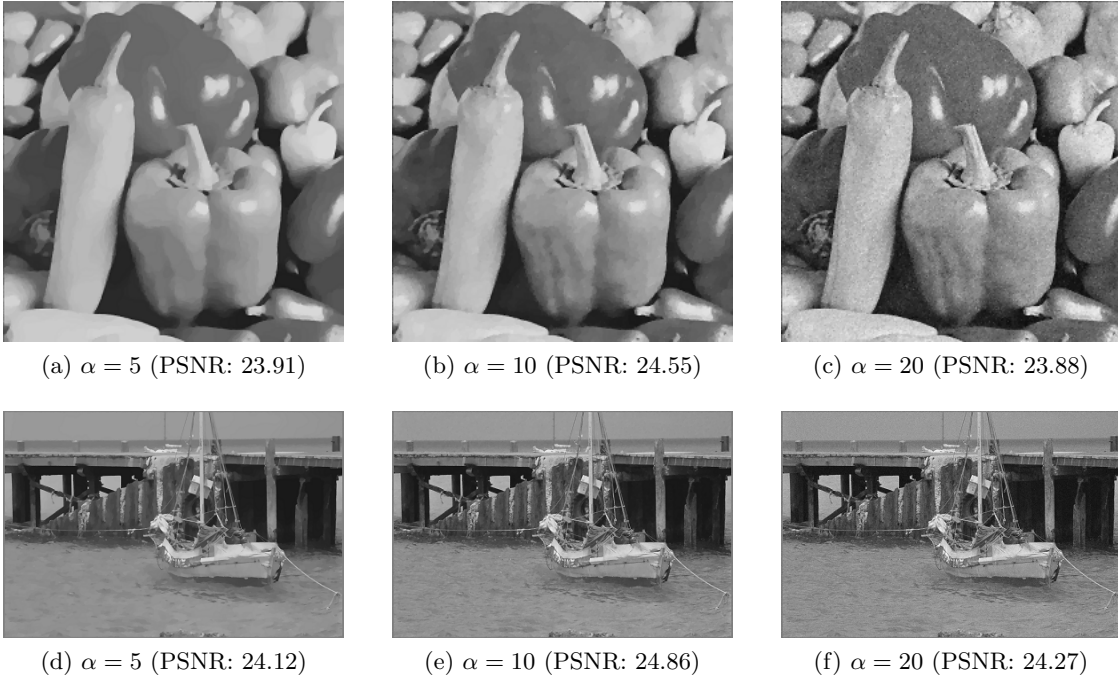


**Figure 5.4.** Results of the fast pre-relaxed block Jacobi method with various values of  $\alpha$  ( $\mathcal{N} = 8 \times 8$ )

Test image	$\alpha$	PSNR	iter	wall-clock time (sec)
Peppers 512 $\times$ 512	5	23.88	26	0.34
	10	24.55	11	0.15
	20	23.91	8	0.12
Boat 2048 $\times$ 3072	5	24.27	94	46.23
	10	24.86	10	7.08
	20	24.12	6	4.64

**Table 5.1**

Performance of the fast pre-relaxed block Jacobi method with various values of  $\alpha$  ( $\mathcal{N} = 8 \times 8$ )

details. In the following experiments, we use

$$(5.1) \quad \frac{F(\mathbf{p}^{(n)}) - F(\mathbf{p}^*)}{F(\mathbf{p}^*)} < 10^{-5}$$

for outer iterations, and

$$\frac{\|\text{div}_s \mathbf{p}_s^{(n+1)} - \text{div}_s \mathbf{p}_s^{(n)}\|_2}{\|\text{div}_s \mathbf{p}_s^{(n+1)}\|_2} < 10^{-4} \quad \text{or} \quad n = 50,$$

for local problems.



Test image	$\mathcal{N}$	PSNR	iter	wall-clock time (sec)
Peppers 512 × 512	1	24.55	-	0.71
	2 × 2	24.55	9	0.70
	4 × 4	24.55	10	0.23
	8 × 8	24.55	11	0.15
	16 × 16	24.55	14	0.20
Boat 2048 × 3072	1	24.86	-	53.24
	2 × 2	24.86	10	50.14
	4 × 4	24.86	10	14.47
	8 × 8	24.86	10	7.08
	16 × 16	24.86	10	4.70

Table 5.2

Performance of the fast pre-relaxed block Jacobi method with various numbers of subdomains  $\mathcal{N}$  ( $\alpha = 10$ )



(a) PSNR: 24.55



(b) PSNR: 24.86

Figure 5.5. Results of the fast pre-relaxed block Jacobi method ( $\mathcal{N} = 16 \times 16$ ,  $\alpha = 10$ )

We compare the results of FPJ with respect to the weight parameter  $\alpha$ . Figure 5.4 shows the results of FPJ with  $\alpha = 5, 10$ , and 20 with  $\mathcal{N} = 8 \times 8$ . As it is well-known for the ROF model, the staircase effect becomes strong as  $\alpha$  decreases. Among three results,  $\alpha = 10$  gives the highest PSNR. We observe from Table 5.1 that both the number of FPJ iterations and the wall-clock time increase as  $\alpha$  decreases.

Table 5.2 shows the performance of FPJ with various numbers of subdomains  $\mathcal{N}$  when  $\alpha = 10$ . The case  $\mathcal{N} = 1$  presents the results of FISTA applied to the full-dimension problem for (2.2) using the stopping criterion (5.1). In the case of the test image “Peppers 512 × 512,” the wall-clock time of FPJ decreases as  $\mathcal{N}$  grows from 1 to 8 × 8, but increases when  $\mathcal{N}$  becomes 16 × 16. It is because the size of “Peppers 512 × 512” is so small that the portion of communication time between processors in the wall-clock time is not negligible compared to computation time if we use  $\mathcal{N} = 16 \times 16$  subdomains. For a sufficiently large test image “Boat 2048 × 3072,” the wall-clock time of FPJ decreases as  $\mathcal{N}$  increases. It shows the efficiency of FPJ as a parallel solver for large-scale images. We also observe numerically that the number

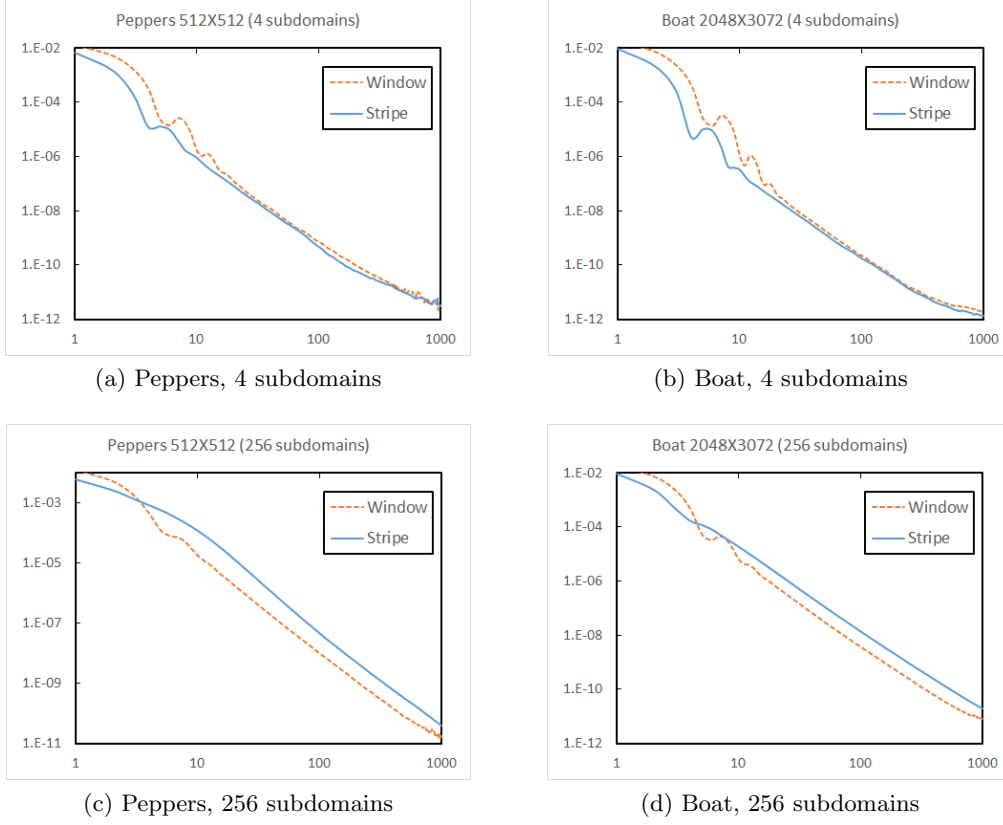


**Figure 5.6.** Decay of  $\frac{F(\mathbf{p}^{(n)}) - F(\mathbf{p}^*)}{F(\mathbf{p}^*)}$  in the fast pre-relaxed block Jacobi method with window/stripe-shaped domain decompositions ( $\alpha = 10$ )

of FPJ iterations increases as  $\mathcal{N}$  grows. Figure 5.5 shows the denoised test images by FPJ with  $\mathcal{N} = 16 \times 16$ . As they show no trace of the subdomain interfaces and have the same PSNR as the case  $\mathcal{N} = 1$ , we can say that FPJ correctly solves (2.2) and recovers images.

Finally, we compare the convergence rate of FPJ for the window-shaped domain decomposition and the stripe-shaped one. Figure 5.6 shows the decay of  $\frac{F(\mathbf{p}^{(n)}) - F(\mathbf{p}^*)}{F(\mathbf{p}^*)}$  for both domain decompositions when  $\mathcal{N} = 4$  and 256. Since  $N_c = 2$  for the stripe shape and  $N_c = 3$  for the window shape, the stripe-shaped domain decomposition converges faster than the window-shaped one when  $\mathcal{N} = 4$ . However, since the total lengths of the subdomain interfaces are  $O(\mathcal{N}^{1/2})$  and  $O(\mathcal{N})$  for the window and stripe shape, respectively, as we observed in Remark 3.9, the window-shaped domain decomposition is faster than the stripe-shaped one when  $\mathcal{N}$  is large enough; see Figure 5.6(c) and (d). Table 5.3 provides the performance of FPJ with the stripe-shaped domain decomposition with various values of  $\mathcal{N}$  when  $\alpha = 10$ . Comparing Tables 5.2 and 5.3, it can be inferred that if  $\mathcal{N}$  is small, the stripe-shaped domain decomposition is more efficient than the window-shaped one, and if  $\mathcal{N}$  is large enough, the opposite holds.



Test image	$\mathcal{N}$	PSNR	iter	wall-clock time (sec)
Peppers $512 \times 512$	1	24.55	-	0.71
	4	24.55	7	0.57
	16	24.55	8	0.22
	64	24.55	13	0.19
	256	24.55	23	1.05
Boat $2048 \times 3072$	1	24.86	-	53.24
	4	24.86	7	37.54
	16	24.86	7	10.53
	64	24.86	9	6.86
	256	24.86	14	7.01

Table 5.3

Performance of the fast pre-relaxed block Jacobi method with various numbers of subdomains  $\mathcal{N}$ , the stripe-shaped case ( $\alpha = 10$ )

**6. Conclusion.** We proved the  $O(1/n)$  convergence rate of the nonoverlapping relaxed block Jacobi method for the dual ROF model proposed in [14]. Then, incorporating the FISTA acceleration technique [2] into this method, we proposed the  $O(1/n^2)$  convergent fast pre-relaxed block Jacobi method. We implemented various block decomposition methods and showed that the fast pre-relaxed block Jacobi method outperforms others numerically. The fast pre-relaxed block Jacobi method also showed good performance as a parallel solver for large-scale images.

Since our convergence analysis cannot be applied directly to overlapping cases, we plan to investigate ways to extend our acceleration methodology to overlapping methods [8] in our future work. In addition, to design scalable DDMs, construction of the coarse grid correction will be considered.

## REFERENCES

- [1] A. BECK AND M. TEBoulLE, *Fast gradient-based algorithms for constrained total variation image denoising and deblurring problems*, IEEE Trans. Image. Process., 18 (2009), pp. 2419–2434.
- [2] A. BECK AND M. TEBoulLE, *A fast iterative shrinkage-thresholding algorithm for linear inverse problems*, SIAM J. Imaging Sci., 2 (2009), pp. 183–202.
- [3] A. BECK AND L. TETRUSHVILI, *On the convergence of block coordinate descent type methods*, SIAM J. Optim., 23 (2013), pp. 2037–2060.
- [4] L. M. BREGMAN, *The relaxation method of finding the common point of convex sets and its application to the solution of problems in convex programming*, USSR Comp. Math. Math. Phys., 7 (1967), pp. 200–217.
- [5] A. CHAMBOLLE, *An algorithm for total variation minimization and applications*, J. Math. Imaging Vision, 20 (2004), pp. 89–97.
- [6] A. CHAMBOLLE AND T. POCK, *A first-order primal-dual algorithm for convex problems with applications to imaging*, J. Math. Imaging Vision, 40 (2011), pp. 120–145.
- [7] A. CHAMBOLLE AND T. POCK, *A remark on accelerated block coordinate descent for computing the proximity operators of a sum of convex functions*, SMAI J. Comput. Math., 1 (2015), pp. 29–54.
- [8] H. CHANG, X.-C. TAI, L.-L. WANG, AND D. YANG, *Convergence rate of overlapping domain decomposi-*

- tion methods for the Rudin-Osher-Fatemi model based on a dual formulation, *SIAM J. Imaging Sci.*, 8 (2015), pp. 564–591.
- [9] P. L. COMBETTES AND V. R. WAJS, *Signal recovery by proximal forward-backward splitting*, *Multiscale Model. Simul.*, 4 (2005), pp. 1168–1200.
  - [10] M. FORNASIER, A. LANGER, AND C.-B. SCHÖNLIEB, *A convergent overlapping domain decomposition method for total variation minimization*, *Numer. Math.*, 116 (2010), pp. 645–685.
  - [11] M. FORNASIER AND C.-B. SCHÖNLIEB, *Subspace correction methods for total variation and  $l_1$ -minimization*, *SIAM J. Numer. Anal.*, 47 (2009), pp. 3397–3428.
  - [12] T. GOLDSTEIN AND S. OSHER, *The split Bregman method for  $L_1$ -regularized problems*, *SIAM J. Imaging Sci.*, 2 (2009), pp. 323–343.
  - [13] M. HINTERMÜLLER AND A. LANGER, *Subspace correction methods for a class of nonsmooth and nonadditive convex variational problems with mixed  $L^1/L^2$  data-fidelity in image processing*, *SIAM J. Imaging Sci.*, 6 (2013), pp. 2134–2173.
  - [14] M. HINTERMÜLLER AND A. LANGER, *Non-overlapping domain decomposition methods for dual total variation based image denoising*, *J. Sci. Comput.*, 62 (2015), pp. 456–481.
  - [15] A. LANGER, S. OSHER, AND C.-B. SCHÖNLIEB, *Bregmanized domain decomposition for image restoration*, *J. Sci. Comput.*, 54 (2013), pp. 549–576.
  - [16] C.-O. LEE, J. H. LEE, H. WOO, AND S. YUN, *Block decomposition methods for total variation by primal-dual stitching*, *J. Sci. Comput.*, 68 (2016), pp. 273–302.
  - [17] C.-O. LEE AND C. NAM, *Primal domain decomposition methods for the total variation minimization, based on dual decomposition*, *SIAM J. Sci. Comput.*, 39 (2017), pp. B403–B423.
  - [18] C.-O. LEE, C. NAM, AND J. PARK, *Domain decomposition methods using dual conversion for the total variation minimization with  $L^1$  fidelity term*, *J. Sci. Comput.*, 78 (2019), pp. 951–970.
  - [19] C.-O. LEE, E.-H. PARK, AND J. PARK, *A finite element approach for the dual Rudin–Osher–Fatemi model and its nonoverlapping domain decomposition methods*, *SIAM J. Sci. Comput.*, 41 (2019), pp. B205–B228.
  - [20] A. QUARTERONI AND A. VALLI, *Domain Decomposition Methods for Partial Differential Equations*, Oxford University Press, New York, 1999.
  - [21] R. T. ROCKAFELLAR, *Convex Analysis*, Princeton University Press, New Jersey, 2015.
  - [22] L. I. RUDIN, S. OSHER, AND E. FATEMI, *Nonlinear total variation based noise removal algorithms*, *Phys. D*, 60 (1992), pp. 259–268.
  - [23] R. SHEFI AND M. TEBoulLE, *On the rate of convergence of the proximal alternating linearized minimization algorithm for convex problems*, *EURO J. Comput. Optim.*, 4 (2016), pp. 27–46.
  - [24] A. TOSELLI AND O. WIDLUND, *Domain Decomposition Methods-Algorithms and Theory*, vol. 34, Springer, Berlin, 2005.
  - [25] P. TSENG, *Convergence of a block coordinate descent method for nondifferentiable minimization*, *J. Optim. Theory Appl.*, 109 (2001), pp. 475–494.
  - [26] Y. WANG, J. YANG, W. YIN, AND Y. ZHANG, *A new alternating minimization algorithm for total variation image reconstruction*, *SIAM J. Imaging Sci.*, 1 (2008), pp. 248–272.
  - [27] C. WU AND X.-C. TAI, *Augmented Lagrangian method, dual methods, and split Bregman iteration for ROF, vectorial TV, and high order models*, *SIAM J. Imaging Sci.*, 3 (2010), pp. 300–339.